Available online at www.sciencedirect.com
SCIENCE DIRECT®
Surface Science 552 (2004) 27–34
SURFACE SCIENCE
www.elsevier.com/locate/susc

CO adsorption on oxide supported gold: from small clusters to monolayer islands and three-dimensional nanoparticles

C. Lemire, R. Meyer, Sh.K. Shaikhutdinov *, H.-J. Freund

Department of Chemical Physics, Fritz-Haber-Institute der Max-Plank-Gesellschaft, Faradayweg 4-6, 14195 Berlin, Germany

Received 16 October 2003; accepted for publication 13 January 2004

Abstract

CO adsorption on gold vapor-deposited on a thin FeO(1 1 1) film grown on a Pt(1 1 1) has been studied with temperature programmed desorption (TPD) and infrared reflection absorption spectroscopy (IRAS). Structural characterization has been performed with scanning tunneling microscopy. Both TPD and IRAS results clearly show a particle size effect such that small Au deposits adsorb CO more strongly. This effect is only observed at low temperature deposition and vanishes after annealing to 500 K. However, the interaction of CO with Au monolayer islands, formed at a low Au coverage, and relatively large three-dimensional particles, formed at higher coverages, is found to be essentially similar. It is proposed that the adsorption of CO only involves low coordinated atoms and is consequently independent of the particles dimensions. The particle size effects are therefore attributed not to quantum size effects but rather to the presence of highly uncoordinated gold atoms in very small particles.

Keywords: Gold; Carbon monoxide; Chemisorption; Clusters; Iron oxide

1. Introduction

In recent years, highly dispersed gold has been shown to be an active catalyst for the low temperature CO oxidation reaction [1–3]. However, a still open question remains as to why gold, which is considered to be the most inert amongst metals, catalyses the CO oxidation reaction when its dimension goes to a nanometer scale.

In order to study the effect of size on the reactivity of metal particles, well-defined model systems have been developed where the particle size and structure of the support can be controlled under vacuum conditions [4–6]. Goodman's group demonstrated that gold particles of ~3 nm supported on TiO_2(1 1 0) showed a maximum in CO oxidation activity [7,8]. Using scanning tunneling spectroscopy, this size effect was related to the observation of the onset of a band gap. The authors suggested that supported metal clusters may have unusual catalytic properties as one dimension of the cluster becomes smaller than three atomic spacings due to the quantum size effect. However, in recent work on the Au/FeO(1 1 1) system we have shown that monolayer islands do not in fact

* Corresponding author. Tel.: +49-030-84134193; fax: +49-030-84134105.
E-mail address: shaikhutdinov@fhi-berlin.mpg.de (S.K. Shaikhutdinov).

0039-6028/$ - see front matter © 2004 Elsevier B.V. All rights reserved.
doi:10.1016/j.susc.2004.01.029

adsorb CO differently from large particles, implying that quantum size effects do not control the low temperature CO oxidation reaction [9]. Meanwhile, theoretical investigations have found that the undercoordinated gold atoms have a remarkable effect on CO adsorption: kinks and steps on gold surfaces provide favorable adsorption sites for CO and oxygen alike [10,11]. Nørskov and co-workers [12] have calculated that the adsorption strength of CO is very sensitive to the coordination number (N) of the gold atoms. Gold nanowires, with $N = 2$, possess a CO binding energy of nearly 4 times greater than that of CO adsorbed on Au(1 1 1) terraces ($N = 9$), which adsorb CO only weakly.

In a recent paper [13], we have reported temperature programmed desorption (TPD) results showing that gold particles supported on alumina and iron oxide films exhibit a size effect such that very small gold particles adsorb CO more strongly. In this work, combining TPD, infrared reflection absorption spectroscopy (IRAS), and scanning tunneling microscopy (STM), we examine the relationship between structure and the adsorption behavior of gold deposits on an FeO(1 1 1) thin film support.

2. Experimental

The experiments were performed in two separate UHV chambers (base pressure below 2×10^{-10} mbar). Both chambers were equipped with Auger electron spectroscopy, low energy electron diffraction (AES, LEED, Omicron), and also with standard facilities for sample cleaning and heating. One chamber was equipped with IR-spectrometer (Mattson RS-1 FTIR, spectral resolution 2 cm^{-1}). The second was used for structural characterization by STM (Omicron). Additionally, both chambers were equipped with differentially pumped mass spectrometers (Hiden Analytical) for TPD measurements such that the TPD spectra could be used for combining the structural and spectroscopic data obtained.

A chromel–alumel thermocouple was spot welded to the edge of the crystal. In both chambers the Pt(1 1 1) crystal of 10 mm in diameter was mounted to a sample holder to provide conductive cooling down to ~90 K by use of liquid nitrogen. Heating was performed by electron bombardment from a tungsten filament placed close to the back side of the crystal.

CO (99.999%) and O_2 (99.999%) (AGA Gas) exposures were performed with a directional doser. For metal (Fe (99.99%), Au (99.99%), Goodfellows) deposition, we used commercial metal evaporators (Focus EFM3). Note that, during evaporation, a retarding potential was applied to the sample to avoid any sputtering caused by acceleration of the metal ions toward the sample.

Thin FeO(1 1 1) films were prepared according to a recipe described elsewhere ([14] and references therein). In brief, ~1 ML of iron is evaporated onto a Pt(1 1 1) single crystal at 300 K and subsequently oxidized at 10^{-6} mbar of O_2 at 1000 K for 2 min.

Gold on the FeO film was deposited with the rate of ca. 0.1 Å min^{-1} as calibrated by a quartz microbalance. The Au coverage is measured in nominal thickness (in Å). For each Au/FeO sample, new films were grown.

For TPD measurements, the sample was placed about 0.5 mm in front of the mass spectrometer shield with 6 mm aperture and heated with a rate of 5 K s^{-1}. Exposure of the sample to CO did not result in any CO_2 formation and the oxide support did not suffer from reduction.

The IRAS measurements were performed at 90 K. In order to increase signal-to-noise ratio, an IRAS spectrum is usually divided to a reference spectrum taken for the same sample prior to gas exposure. However, we have observed that small amounts of CO may adsorb during gold deposition from the vacuum background as shown in the blank experiment by taking TPD spectra without exposing the sample to CO. As a result, the most strongly bound state can be partially populated prior to CO adsorption experiments. These CO molecules cannot be thermally desorbed without changing morphology, as the TPD spectra are found to be irreversibly changed upon heating (see below). Therefore, in order to study CO adsorption on Au deposits formed at 90 K, we have also used a spectrum for the clean FeO film taken before deposition as a reference, bearing in mind that

the FeO surface does not adsorb CO under these conditions.

All STM images were taken at room temperature with commercial Pt–Ir tips at typical bias and current of 2–100 mV and 0.5–1 nA, respectively. The images were found to be independent of a bias polarity.

3. Results and discussion

The FeO film typically showed wide flat terraces separated by monoatomic steps of ~2.5 Å high corresponding to the Pt(1 1 1) substrate underneath the film. The surface exhibits a characteristic Moiré structure formed by a 10% mismatch between FeO(1 1 1) and Pt(1 1 1) lattices and can be clearly seen in LEED patterns [15]. The STM images reveal a honeycomb superstructure with a ~26 Å periodicity in turn exhibiting an atomic structure with a ~3 Å lattice constant (see inset in Fig. 1a). In addition, a small number of "holes" in the film can be observed which expose clean or oxygen covered Pt(1 1 1) (one is marked by arrow in Fig. 1b). No point defects such as vacancies were detected in the high resolution STM images.

After deposition at 120 K, gold was seen to first decorate substrate steps and holes as previously reported [13]. Subsequently, gold nucleates at the terraces as well, forming small clusters and their aggregates as shown in Fig. 1a.

At gold coverage of 0.1–0.2 Å, gold forms islands primarily one atomic layer in height, which are homogeneously distributed on the terraces. The atomically resolved STM images revealed that the gold islands consist of a single Au(1 1 1) layer as shown in the inset in Fig. 1b. The atomic rows of gold within the island are parallel to those of the support, thus indicating that the layer of Au atoms is in good epitaxial relationship with the oxide support, i.e., similar to what we have recently observed for Pd on FeO(1 1 1) [16]. However, unlike the case of Pd where large monolayer islands can be formed over the entire surface upon annealing, islands of two Au layers develop on the surface at 0.3 Å coverage as shown in Fig. 1c. Therefore, the gold–gold interaction prevails over the interaction with the FeO(1 1 1) support, which

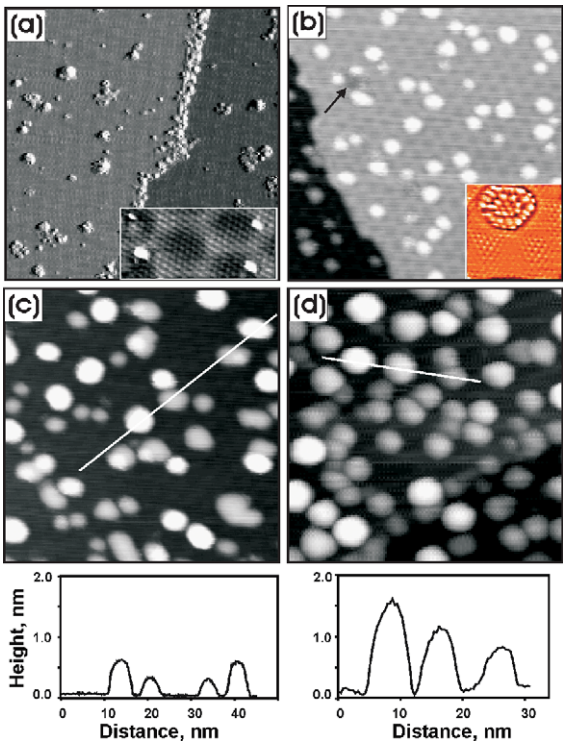

Fig. 1. Room temperature STM images of the Au/FeO(1 1 1)/Pt(1 1 1) surfaces at a different gold coverage: 0.05 Å (a), 0.2 Å (b), 0.3 Å (c) and 2 Å (d) (all images are 50×50 nm^2). The samples except (a) were annealed to 500 K after deposition at 120 K. The inset in (a) show the atomically resolved support structure with few small clusters formed (image size is 7×3.5 nm^2). All particles in the image (b) are monolayer islands of ~2.5 Å high and show up a Au(1 1 1) single layer as resolved in inset (size 5×5 nm^2). The arrow in (b) indicates the hole present in the film. The heights of the particles imaged in (c) and (d) are shown in the profiles along the white lines, showing that particles starts to grow in a 3D mode by increasing the number of (1 1 1) layers at increasing coverage. Note that the image (a) and insets are presented with a differentiated contrast.

in turn seems to be much weaker than for Pd/FeO. As a result, the transition from a two- to three-dimensional (3D) growth mode occurs at a very low coverage. Note that similar behavior has been seen for the growth of gold particles on TiO_2(1 1 0) [17–21].

At further increasing coverage, the particle size grows such that, at highest coverage studied (~2 Å), Au deposits represent particles up to 7 nm in diameter and five layers in height as shown in Fig. 1d. Recalling our finding that Au(1 1 1) monolayer

islands are formed at a lower coverage, it seems likely that Au particles grow by increasing the number of (1 1 1) layers as has been seen for large gold particles on TiO_2 [22] and on mica [23].

In Fig. 2a, the CO TPD spectra for gold particles as deposited at 90 K show that as Au coverage increases, the CO desorption temperature decreases, indicating a particle size effect. For the smallest gold coverage, the presence of a state with desorption temperatures out to 300 K is clearly seen, which has never been observed for Au crystalline surfaces. Fig. 2b shows that annealing the gold particles to 500 K results in a loss of signal intensity (by factor of ~2) and a shift of the high temperature desorption peak to lower temperature. (Note that no further spectra changes were found in subsequent TPD experiments after initial annealing.) The annealing effects can be understood in terms of sintering of the small clusters on heating and restructuring of the growing Au particles such that the particles become more ordered [13].

The decrease in CO chemisorption following sintering of gold particles has been observed for gold catalysts [24–26] due to the loss of surface area. The effects of restructuring have also been well documented as gold films deposited at low temperatures have been seen to adsorb significantly more CO than the smooth films formed at higher temperature deposition [27–30]. Furthermore, in a reverse experiment, Gottfried et al. have recently found that roughening of an Au(1 1 0) crystal by Ar^+ bombardment gives rise to new desorption states around 185 and 230 K that are not seen on the smooth surface [31], presumably due to the decreased coordination of the surface atoms on the sputtered surface. Therefore, we believe that the shift of the high temperature desorption feature results from the loss of low coordinated gold atoms which have been theoretically predicted to adsorb CO more strongly [10–12].

Fig. 2b shows that the CO desorption features observed at around 130 and 200 K for the annealed samples are independent of the Au coverage, indicating that even monolayer islands (see Fig. 1b) show similar desorption spectra features as large particles, which are in turn quite similar to those observed on the Au(3 3 2) single crystal surface [32].

To complement the TPD experiments, the nature of the CO adsorption states on gold deposits has been studied with IRAS. Fig. 3 shows IRAS

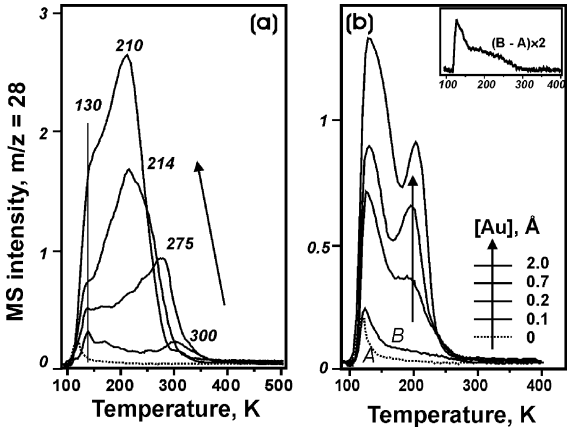

Fig. 2. The first (a) and second (b) CO TPD spectra of Au/FeO(1 1 1) after exposure to 1.5 L CO at 90 K as a function of gold coverage (in Å). Gold deposition was performed at 90 K. Note that the signal intensity decreases by factor of ~2 after initial annealing and is not changed upon further TPD runs. The CO TPD spectrum on bare FeO(1 1 1) is also plotted by dash line. The small feature at ~120 K has been assigned to CO desorbing from the sample holder as no any signal has been detected on the clean FeO by IRAS. The inset in (b) show the difference spectrum at a lowest coverage for clarity.

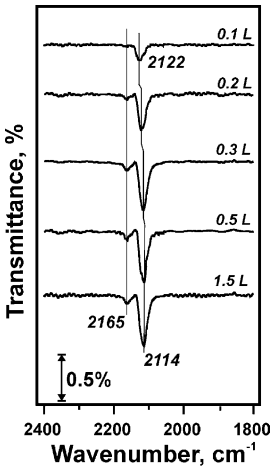

Fig. 3. CO IRAS spectra of Au/FeO(1 1 1) as a function of CO exposure (1 L = 10^{-6} mbar s) at 90 K (gold coverage = 0.2 Å, deposition temperature is 90 K).

spectra for the sample possessing 0.2 Å of gold deposited at 90 K. The first spectrum taken immediately after gold deposition shows a peak at 2122 cm^{-1} assigned to strongly adsorbed CO on the unstructured particles from the vacuum background. With increasing CO exposure, the main peak grows and shifts to 2114 cm^{-1}, and in addition a small feature at 2165 cm^{-1} emerges. Similar behavior is observed for other samples at low Au coverages (0.1–0.7 Å): the main peak shifts to lower wavenumbers and the small feature centered at 2165 cm^{-1} only develops at higher CO exposure. This indicates that the signal at 2165 cm^{-1} corresponds to more weakly bound CO, meanwhile, the main peak must be attributed to the most strongly bound state observed in TPD spectra shown in Fig. 2a.

Although the red shift of the lower frequency feature at increasing CO coverage is atypical of CO adsorption on other metal surfaces such as Pt or Pd [33,34], this trend is well known for CO adsorption on coinage metals (Cu, Ag, Au) [29,35,36]. This behavior is generally attributed to the lack of back donation of electrons from the metal d states into the $2\pi^*$ orbital of CO [35,36]. Therefore, bonding is dominated by the 5 orbital and as the coverage increases, the degree of donation from CO to the metal will decrease, leading to a red shift [36–38].

Fig. 4a shows the IRAS spectra taken at saturated CO exposure for samples deposited at 90 K as a function of gold nominal thickness. At a coverage of 0.1 Å, the two features described before are observed with nearly equal intensity. With increasing coverage, the higher frequency peak (at 2165 cm^{-1}) decreases before disappearing at about 2 Å of Au, while the main feature gradually grows and shifts to lower wavenumbers from 2131 to 2108 cm^{-1}. This trend is different than that observed by previous researchers examining gold particles on thin alumina films [39,40], where CO adsorbed on the smallest particles was observed to be at lower wavenumbers (~2100 cm^{-1}) and shifted to 2110 cm^{-1}, the characteristic value for metallic (bulk) gold [29,41], as the particle size increased. Also, Heiz and co-workers [42] have observed for Au_8 clusters supported on a MgO thin film that the CO stretching frequency (2102

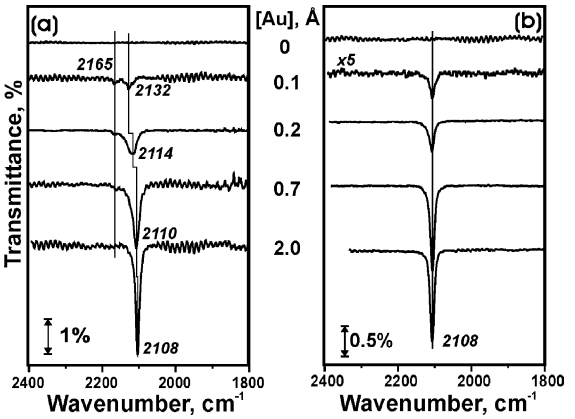

Fig. 4. The IRAS spectra of 1.5 L CO adsorbed on Au/FeO(1 1 1) at 90 K as a function of gold coverage for the samples as deposited at 90 K (a) and those annealed to 500 K (b). The corresponding CO TPD spectra are shown in Fig. 2.

cm^{-1}) is red-shifted slightly from the value for bulk gold. One may suggest that the origin of the differences between our system and these examples is associated with differences in the growth mode of gold on these surfaces, which is three-dimensional from the onset on MgO and alumina films, and two-dimensional on FeO(1 1 1) at low coverages. In fact, Goodman's group has recently studied CO adsorption on Au particles on a TiO_2 thin film, whereby Au grows in a 2D-mode at low coverages, and also observed adsorption frequencies higher (2116–2126 cm^{-1}) than that of CO adsorbed on bulk gold [43]. However, as we have found that monolayer islands of only 2–3 nm in diameter exhibit the same adsorption behavior as bulk gold, the blue shift for the smallest particles cannot be simply ascribed to the presence of 2D-particles.

As shown in Fig. 4b, annealing to 500 K results in the observation of a single state at 2108 cm^{-1} independent of the Au coverage with a disappearance of the state at 2165 cm^{-1}, just as in the case of high gold coverage. The feature at 2108 cm^{-1} can be straightforwardly assigned to metallic gold in agreement with previous results [29,32,41]. A higher wavenumber of CO stretching band compared to CO in gas phase (2143 cm^{-1}) is usually an indication that CO species is interacting with electron-deficient sites. Therefore, we propose that the feature at 2165 cm^{-1} arises from CO adsorbed on small gold clusters, which can undergo

charge transfer due to a specific interaction with the support. In previous IRAS studies on different catalysts systems, such as gold supported on zeolites [44], ZrO_2 [45], TiO_2 [45–47] and Fe_2O_3 [48,49], similar frequencies have been also detected and assigned to CO adsorbed on Au^+ species [44,49] or on Au that is interacting with hydroxyl groups on the support [45,46,48]. One possible explanation for such a particle-support interaction in our systems prepared by metal vapour deposition arises from defects of the support. However, oxygen vacancy defects, which act as nucleation centers for Au/TiO_2 [50–52], are not observed in the high resolution STM images of FeO(1 1 1) films and the nucleation seems to occur in a non-preferential way on the regular surface [16,53]. As we have observed that early nucleation is favorable on steps or on the holes present in the film [13], one could logically assign the signal at 2165 cm^{-1} to CO adsorbed on gold nucleating at these features. However, in the case of annealed samples which also possess a high number of particles at the steps, the high frequency state has vanished. Since annealing induces agglomeration of gold and the formation of larger particles, the charge may be effectively screened. Naturally, increasing the Au coverage also favors growth of larger particles, which could result in the screening of the charge as well. This means that whatever the source of the Au^+ feature observed, it likely stems from extremely small gold clusters. Speculatively, we assign the feature at 2165 cm^{-1} to CO adsorbed on very small gold clusters (or even single atoms) that are in some way interacting with oxygen, either by their presence at steps or on the oxygen filled holes (i.e., O/Pt) of the film.

As mentioned above, the Au^+ feature appears after the main peak observed at lower wavenumbers (see Fig. 3), which we have assigned to CO strongly bound on metallic Au clusters. This implies that CO adsorbs on Au^+ species more weakly than on the metal clusters and therefore desorbs in a broad low temperature signal in the corresponding TPD spectra shown in Fig. 2a. This finding is in apparent contradiction with the view of some investigators that charged gold adsorbs CO more strongly [25,49,54]. However, in agreement with our results, Fan et al. have recently found that Au/TiO_2 catalysts with metallic gold chemisorbed CO more effectively than samples with oxidic gold [55].

Fig. 4 shows that for the largest Au coverage studied (2 Å), the position of the desorption peaks in the TPD spectra and of the single peak in IRAS spectra are similar for annealed and non-annealed samples. In contrast, for sub-monolayer Au coverages, two states are observed in IRAS spectra of as deposited particles. However, after annealing, both the TPD and IRAS spectra show the same behavior as the larger particles. Therefore, it seems likely that there is a critical size of gold (or atomic coordination number) above which the CO adsorption properties are essentially identical and not much affected by annealing.

By calibrating mass spectrometer, we have calculated how many CO molecules adsorb on the sample showing Au monolayer islands in STM images (see Fig. 1b). It turns out that only about 10 CO molecules are adsorbing at 90 K per Au monolayer islands of 2 nm in average diameter, i.e. consisting of ca. 50 gold atoms. This finding strongly indicates that CO adsorbs on Au atoms at the metal/support periphery rather than on top of Au(1 1 1) layer. Moreover, if we deconvolute the TPD signal in low and high temperature states, then we find that, on average, only about five CO molecules per island are responsible for adsorption on the most strongly bound state. Therefore, the high temperature state in CO TPD spectra could be assigned to adsorption on more "unsaturated" corner Au atoms. As far as low temperature state is concerned, we have recently shown that this state is "invisible" in IRAS [9], which leads to observation of only a single peak in IRAS spectra while TPD reveals two states (see Figs. 2b and 4b). Due to the selection rules applied to IRAS method, we have suggested that it could be associated with CO molecules laying flat on the gold surface or strongly tilted.

4. Conclusions

The adsorption of CO on FeO(1 1 1) supported gold particles was studied as function of the Au coverage and the substrate temperature by TPD

and IRAS. Both techniques have shown a particle size effect such that small Au deposits adsorb CO more strongly. The effect vanishes upon heating to 500 K, however, the interaction of CO with annealed gold deposits is remarkably similar regardless of particle thickness. Therefore, quantum size effects are not likely to be the controlling factor in the adsorption of CO on gold nanoparticles. The presence of particle size effects in systems as deposited at low temperatures suggests instead that the exceptional activity of gold nanoparticles and size and support effects seen in CO oxidation on real catalytic systems probably arise from the presence of highly uncoordinated atoms.

Acknowledgements

We acknowledge the EU Training Networks "Catalysis by Gold" (TMR Auricat) and "Reactivity of clean and modified oxide surfaces" (TMR Marceille). RJM thanks the Alexander von Humboldt Foundation for a fellowship.

References

[1] M. Haruta, M. Date, Appl. Catal. A 222 (2001) 427.
[2] M. Haruta, CATTECH 6 (2002) 102.
[3] G.C. Bond, D.T. Thompson, Catal. Rev. Sci. Eng. 41 (1999) 319.
[4] C.T. Campbell, Surf. Sci. Rep. 27 (1997) 1.
[5] A.K. Santra, D.W. Goodman, J. Phys.: Condens. Matter 14 (2002) R31.
[6] M. Bäumer, H.-J. Freund, Prog. Surf. Sci. 61 (1999) 127.
[7] M. Valden, X. Lai, D.W. Goodman, Science 281 (1998) 1647.
[8] M. Valden, S. Pak, X. Lai, D.W. Goodman, Catal. Lett. 56 (1998) 7.
[9] C. Lemire, R. Meyer, S. Shaikhutdinov, H.-J. Freund, Angew. Chem. Int. Ed. 43 (2004) 118.
[10] Z.P. Liu, P. Hu, A. Alavi, J. Am. Chem. Soc. 124 (2002) 14770.
[11] M. Mavrikakis, P. Stoltze, J. Nørskov, Catal. Lett. 64 (2001) 101.
[12] S.R. Bahn, N. Lopez, J.K. Nørskov, K.W. Jacobsen, Phys. Rev. B 66 (2002) 081405.
[13] S. Shaikhutdinov, R. Meyer, M. Naschitzki, M. Bäumer, H.-J. Freund, Catal. Lett. 86 (2003) 211.
[14] W. Weiss, W. Ranke, Prog. Surf. Sci. 70 (2002) 1.
[15] M. Ritter, W. Ranke, W. Weiss, Phys. Rev. B 57 (1998) 7240.
[16] S. Shaikhutdinov, R. Meyer, D. Lahav, M. Bäumer, T. Klüner, H.-J. Freund, Phys. Rev. Lett. 91 (2003) 076102.
[17] L. Zhang, R. Persaud, T.E. Madey, Phys. Rev. B 56 (1997) 10549.
[18] X. Lai, T.P. St. Clair, M. Valden, D.W. Goodman, Prog. Surf. Sci. 59 (1998) 25.
[19] Q. Guo, K. Luo, K.A. Davis, D.W. Goodman, Surf. Interf. Anal. 32 (2001) 161.
[20] A.K. Santra, A. Kolmakov, F. Yang, D.W. Goodman, Jpn. J. Appl. Phys. 42 (2003) 4795.
[21] S.C. Parker, A.W. Grant, V.A. Bondzie, C.T. Campbell, Surf. Sci. 441 (1999) 10.
[22] F. Cosandey, T. Madey, Surf. Rev. Lett. 8 (2001) 73.
[23] S. Ferrero, A. Piednoir, C.R. Henry, Nanoletters 1 (2001) 227.
[24] M. Maciejewski, P. Fabrizioli, J.D. Grunwaldt, O.S. Becker, A. Baiker, Phys. Chem. Chem. Phys. 3 (2001) 3846.
[25] F. Boccuzzi, G. Cerrato, F. Pinna, G. Strukul, J. Phys. Chem. B 102 (1998) 5733.
[26] F. Boccuzzi, A. Chiorino, M. Manzoli, D. Andreeva, T. Tabakova, J. Catal. 188 (1999) 176.
[27] B. Gleich, M. Ruff, R.J. Behm, Surf. Sci. 386 (1997) 48.
[28] M. Ruff, S. Frey, B. Gleich, R.J. Behm, Appl. Phys. A 66 (1998) S513.
[29] P. Dumas, R.G. Tobin, P.L. Richards, Surf. Sci. 171 (1986) 579.
[30] P. Dumas, R.G. Tobin, P.L. Richards, J. Electron. Spectrosc. Relat. Phenom. 39 (1986) 183.
[31] J.M. Gottfried, K.J. Schmidt, S.L.M. Schroeder, K. Christmann, Surf. Sci. 536 (2003) 206.
[32] C. Ruggiero, P. Hollins, J. Chem. Soc. Faraday Trans. 92 (1996) 4829.
[33] C.W. Olsen, R.I. Masel, Surf. Sci. 201 (1988) 444.
[34] J. Szanyi, W.K. Kuhn, D.W. Goodman, J. Vac. Sci. Techn. A 11 (1993) 1969.
[35] A.M. Bradshaw, J. Pritchard, Proc. Roy. Soc. A 316 (1970) 169.
[36] J. France, P. Hollins, J. Electron. Spectrosc. Relat. Phenom. 64 (1993) 251.
[37] A. Föhlisch, M. Nyberg, P. Beenich, L. Triguero, J. Hasselström, O. Karis, L.G.-M. Pettersson, A. Nilsson, J. Chem. Phys. 112 (2000) 1946.
[38] R.A. van Santen, M. Neurock, Catal. Rev. Sci. Eng. 37 (1995) 557.
[39] D.R. Rainer, C. Xu, P.M. Holmblad, D.W. Goodman, J. Vac. Sci. Techn. A 15 (1997) 1653.
[40] C. Winkler, A.J. Carew, S. Haq, R. Raval, Langmuir 19 (2003) 717.
[41] Y. Jugnet, F.J. Cadete Santos Aires, C. Deranlot, L. Piccolo, J.C. Bertolini, Surf. Sci. 521 (2002) L639.
[42] A. Sanchez, S. Abbet, U. Heiz, W.D. Schneider, H. Häkkinen, R.N. Barnett, U. Landman, J. Phys. Chem. A 103 (1999) 9573.
[43] D.C. Meier, D.W. Goodman, J. Am. Chem. Soc. 126 (2004).

[44] D. Guillemot, V.Y. Boresko, V.B. Kazansky, M. Polisset-Thfoin, J. Fraissard, J. Chem. Soc. Faraday Trans. 93 (1997) 3587.
[45] M. Manzoli, A. Chorino, F. Boccuzzi, Surf. Sci. 532 (2003) 377.
[46] H. Liu, A.I. Kozlov, A.P. Kozlova, T. Shido, K. Asakura, Y. Iwasawa, J. Catal. 185 (1999) 252.
[47] M.A.P. Dekkers, M.J. Lippits, B.E. Nieuwenhuys, Catal. Lett. 56 (1998) 195.
[48] H. Liu, A.I. Kozlov, A.P. Kozlova, T. Shido, Y. Iwasawa, Phys. Chem. Chem. Phys. 1 (1999) 2851.
[49] S. Minicò, S. Scirè, C. Crisafulli, A.M. Visco, S. Galvagno, Catal. Lett. 47 (1997) 273.
[50] E. Wahlström, N. Lopez, R. Schaub, P. Thostrup, A. Rønnau, C. Africh, E. Laegsgaard, J.K. Nørskov, F. Besenbacher, Phys. Rev. Lett. 90 (2003) 026101.
[51] N. Lopez, J.K. Nørskov, Surf. Sci. 515 (2002) 175.
[52] L. Giordano, G. Pacchioni, T. Bredow, J. Fernández Sanz, Surf. Sci. 471 (2001) 21.
[53] R. Meyer, M. Bäumer, Sh.K. Shaikhutdinov, H.-J. Freund, Surf. Sci. 546 (2003) L813.
[54] T.M. Salama, T. Shido, R. Ohnishi, M. Ichikawa, J. Phys. Chem. 100 (1996) 3688.
[55] L. Fan, N. Ichikuni, S. Shimazu, T. Uematsu, Appl. Catal. A 246 (2003) 87.